© 2016. Published by The Company of Biologists Ltd | Development (2016) 143, 1149-1159 doi:10.1242/dev.132886

RESEARCH ARTICLE

Progressive developmental restriction, acquisition of left-right identity and cell growth behavior during lobe formation in mouse liver development

Mary C. Weiss[1,*], Jean-Francois Le Garrec[2], Sabrina Coqueran[1], Helene Strick-Marchand[3] and Margaret Buckingham[1]

ABSTRACT

To identify cell-based decisions implicated in morphogenesis of the mammalian liver, we performed clonal analysis of hepatocytes/hepatoblasts in mouse liver development, using a knock-in allele of *Hnf4a*/*laacZ*. This transgene randomly undergoes a low frequency of recombination that generates a functional *lacZ* gene that produces β-galactosidase in tissues in which *Hnf4a* is expressed. Two types of β-galactosidase-positive clones were found. Most have undergone three to eight cell divisions and result from independent events (Luria–Delbrück fluctuation test); we calculate that they arose between E8.5 and E13.5. A second class was mega-clones derived from early endoderm progenitors, generating many descendants. Some originated from multi-potential founder cells, with labeled cells in the liver, pancreas and/or intestine. A few mega-clones populate only one side of the liver, indicating hepatic cell chirality. The patterns of labeled cells indicate cohesive and often oriented growth, notably in broad radial stripes, potentially implicated in the formation of liver lobes. This retrospective clonal analysis gives novel insights into clonal origins, cell behavior of progenitors and distinct properties of endoderm cells that underlie the formation and morphogenesis of the liver.

KEY WORDS: Mouse liver development, Retrospective clonal analysis, β-Galactosidase reporter, *Hnf4a*-directed expression

INTRODUCTION

The liver of mammals begins as an outgrowth of the embryonic gut, the hepatic diverticulum, at the foregut-midgut junction. This endodermal pouch will give rise to two types of tissue: the rostral portion will become the hepatoblasts/hepatocytes of the liver, and the caudal part will become the intra-hepatic biliary system, composed of cholangiocytes and ductal cells. In the mouse, the newly formed hepatic diverticulum at embryonic day (E) 8.5 invades the septum transversum mesenchyme (STM), where a series of inductive tissue interactions, first described by Le Douarin (1975), result in rapid growth, and changes in cell shape and behavior that permit the diverticulum cells to delaminate and intermingle with cells of the STM. From E9.5, clumps of cells forming liver tissue can be seen within the STM (Kaufman, 1992) and at E11.5 the liver emerges as an organ (Kaufman and Bard, 1999).

[1]CNRS URA 2578, Département Biologie du Développement et Cellules Souches, Institut Pasteur, 25-28 rue du Dr Roux, Paris 75724, Cedex 15, France. [2]Imagine-Institut Pasteur, Heart Morphogenesis Group, Paris 75015, France. [3]Innate Immunity Unit, INSERM U668, Institut Pasteur, Paris 75724, France.

*Author for correspondence (mweiss@pasteur.fr)

Received 10 November 2015; Accepted 10 February 2016

Recent work has made use of transgenic embryos, short-term tissue culture of embryos and explants, and double/triple staining of participating cells to supplement the above description with mechanistic elements. The inductive interactions appear to involve signaling by members of the fibroblast growth factor (FGF) (Gualdi et al., 1996; Jung et al., 1999) and bone morphogenetic protein (BMP) (Rossi et al., 2001) families, emanating from interacting mesenchymal cells of the cardiac mesoderm and STM, respectively. In addition, a number of genes have been identified that encode cell-autonomous factors that are required to accomplish these steps, in particular the Hex homeobox (HHEX) (Martinez Barbera et al., 2000; Bort et al., 2006), PROX1 (Sosa-Pineda et al., 2000), GATA (Rojas et al., 2005) and FOXA (Lee et al., 2005) factors.

During the early stages of liver formation, the endodermal cells are closely associated with the embryonic vitelline veins, which traverse the STM and will be incorporated into the liver tissue and give rise to the blood sinusoids where fetal hematopoiesis occurs (Crawford et al., 2010). During mid-gestation, a significant fraction of the cells in the liver are blood cells (Paul et al., 1969; Golub and Cumano, 2013), and it is only after birth that hematopoiesis moves to its definitive site.

Fate mapping of the early endoderm has been carried out on mouse embryos using a vital dye to mark small clumps of endoderm cells at the anterior intestinal portal. After a short period of culture, groups of labeled cells contributing to the gut tube and the liver bud were found in approximately equal frequencies, whereas those in the pancreas were 20-40 times less frequent, indicating that the progenitor pools are of a similar size for liver and gut, but much smaller for pancreas (Tremblay and Zaret, 2005). This difference in size of the progenitor pools was confirmed by targeted cell ablation during embryogenesis to demonstrate the capacity of liver but not pancreas to achieve compensatory growth to replace cells of the depleted organ (Stanger et al., 2007).

The clonal analysis described here was undertaken to define events occurring during morphogenesis of the mouse liver, specifically in the hepatoblast/hepatocyte population, and beginning with progenitors that are common to the liver, the pancreas and the gut. We aimed to determine when progenitor fate becomes limited to a single tissue and any restrictions that are imposed upon these cells. We planned to deduce the mode of growth at different stages, and aspects of cell behavior: migration patterns, cohesive versus non-cohesive growth, and the possible existence of liver cell fields. To answer these questions, we used a *lacZ* reporter transgene containing a duplication which is removed by a rare and random recombination event (Bonnerot and Nicolas, 1993), and with its expression directed by a tissue-specific promoter (Nicolas et al., 1996). Here, expression of the reporter is directed by the *Hnf4a* gene, coding for a liver-enriched transcription factor,

Development (2016) 143, 1149-1159 doi:10.1242/dev.132886

expressed in liver progenitor cells of the hepatic diverticulum from E8.5 (Duncan et al., 1994).

RESULTS

A strategy for clonal analysis of the mammalian liver

The clonal analysis of liver development began with construction of a reporter transgene under the control of a gene expressed specifically in the hepatoblasts/hepatocytes. As a reporter transgene we chose *n-laacZ* (Bonnerot and Nicolas, 1993), a mutant version of the bacterial *lacZ* gene containing a duplication that introduces a stop codon: no β-galactosidase (β-gal) activity is present unless an intragenic recombination event removes the duplication. This event is rare and random; the only requirement is that descendants of the corrected cells survive and grow. The marker transgene was introduced into the 3′UTR of the *Hnf4a* gene (Fig. 1A); this gene has two alternative promoters (Nakhei et al., 1998) so 3′ localization of the transgene should permit expression from both the P1 and P2 promoters.

Hnf4a is expressed in presumptive liver cells from E8.5 (Duncan et al., 1994) and continues to be expressed in hepatoblast/hepatocyte liver cells throughout the life of the animal. *Hnf4a* is also expressed from mid-gestation in the pancreas, the stomach, the small and large intestine, and the kidney, but not in the intra- or extra-hepatic biliary system (Zhao and Duncan, 2005; Hunter et al., 2007). HNF4α is a transcription factor that is essential for expression of a large number of genes expressed in the liver and is required for embryogenesis (Duncan et al., 1997; Hayhurst et al., 2001). In humans, its mutation leads to a form of adult-onset diabetes (see Sladek, 1993).

The liver as an organ appears rather late during development. It is present at E11.5, and is already delineated into lobes: the left and right medial lobes, located at the rostral pole, and left and right lateral lobes, sitting just underneath. During the following 3 days, the form of the liver remains similar, but by E14.5 the smaller lobes of the right side of the liver, the caudate lobe and the papillary processes begin to develop. Two of the stages are illustrated in Fig. 1B, which presents a four-lobe liver at E13.5 and the more complex appearance of an E15.5 liver.

Clusters in E11.5 to E16.5 embryos: independent events

Embryos were collected after 11.5 to 16.5 days of gestation to allow us to observe the influence of developmental age on the frequency of clone emergence and the evolution with time of the labeled cells (Table 1). At all ages, β-gal$^+$ cells were observed at a low frequency: between 80% (E11.5) and 40% (E16.5) of the embryos contained no marked cells in the liver. When β-gal$^+$ cells were numerous, they were grouped (clustered) together (Fig. 2A-G; Fig. S1). The clusters were evenly divided among the lobes, indicating that emergence is random, occurring throughout the embryonic liver cell population.

The clusters show a clear evolution with age. The liver tissue is relatively transparent at the early stages, but by E13.5 occupation of the liver by hematopoietic cells has made the tissue denser and less transparent. In the youngest embryos, the blue-stained nuclei are small and the staining is light; with age the staining becomes more intense and the nuclei increase in size. This is consistent with the expression levels of *Hnf4a* during development: weakly expressed in the liver diverticulum and increasing throughout development. Within the clusters, the nuclei are evenly dispersed rather than clumped together (Fig. 2; Fig. S1).

Whereas the younger embryos contained usually one cluster per liver located in a single lobe, the older ones often had clusters in different lobes. Fig. 3 displays the lobe occupation of clusters and the cell numbers of the clusters (with colors to indicate the number of calculated cell divisions), with separate groupings for the single-lobe and multi-lobe clusters. This illustrates the shift towards increasing cell numbers of the single-lobe clusters. The small differences in cluster numbers of the different lobes might reflect differential growth in the lobe of origin at the time of emergence of the progenitor cell.

To understand the relationship between cluster origin and clonality, we have used the Luria–Delbrück fluctuation test (Luria and Delbrück, 1943) to determine the probability of more than one independent 'event' in each age group of embryos. An 'event' refers to a recombination in the *nlaacZ* sequence permitting heritable production of an active β-gal protein in any cell and its *Hnf4a*-expressing descendants. Fig. 4 shows the extremely close similarities of the expected and observed frequencies of 0, 1, 2 and >2 events (clusters in one, two or more than two lobes) for E11.5 to E16.5. These results clearly indicate that most of the two- and multiple-lobe clusters result from independent recombination events.

We conclude that liver cells in which the *laacZ* duplication has been recombined to give a functional *lacZ* emerged at the

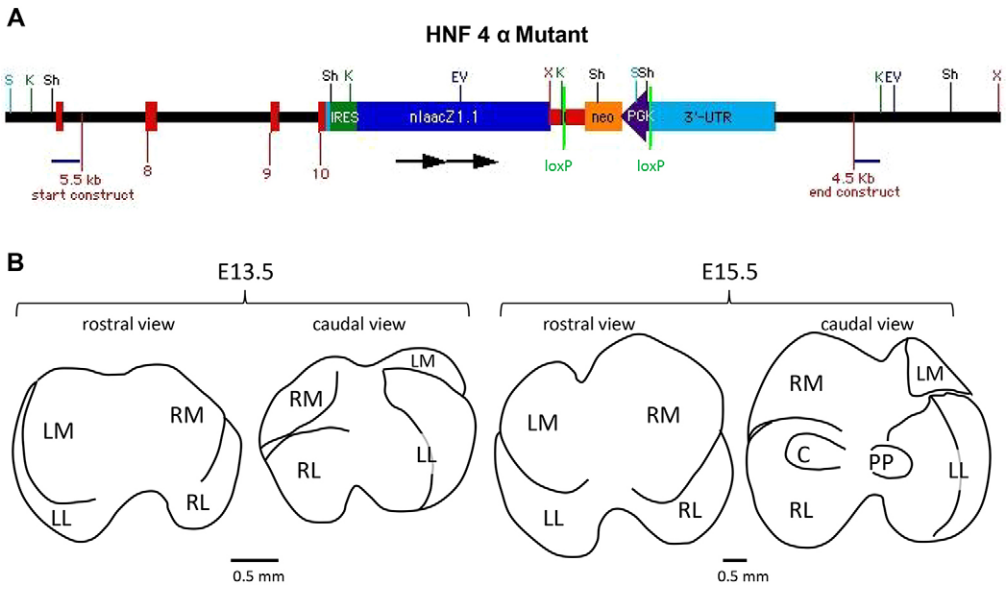

Fig. 1. Knock-in *Hnf4a* allele and embryonic mouse liver structure. (A) Scheme of the construct used to introduce the *nLaacZ* sequence into the 3′ UTR of the *Hnf4a* gene. Restriction sites are indicated; the terminal exons are presented as red boxes on the left; loxP sites are green. Black arrows indicate the duplication in the *nlaacZ* gene. (B) Drawings of the appearance of the embryonic liver at E13.5 and E15.5, presented from the rostral and caudal views. At E13.5, there is a simple four-lobe structure; from the caudal view the edges of the right medial (RM) and left medial (LM) lobes are folded over. At E15.5 the structure is similar, but the beginnings of the right caudate (C) lobe and the papillary process (PP) are visible near the midline on the caudal side. LL, left lateral lobe; RL, right lateral lobe.

Development (2016) 143, 1149-1159 doi:10.1242/dev.132886

Table 1. Embryonic age and number of embryos examined

Embryonic day	Number of embryos examined	Proportion unlabeled
E11.5	24	0.83
E12.5	67	0.85
E13.5	177	0.77
E14.5	15	0.73
E15.5	48	0.4
E16.5	71	0.41

anticipated low frequency (Table 1), which is a prerequisite for obtaining statistically significant frequency data and which provided the clear indication that clustered cells are descendants of single progenitor cells, resulting from clonal events.

Comparison of cell clusters on the surface and within the lobes in E16.5 embryos

This technique of retrospective clonal analysis has been used mainly for tissues that are sufficiently thin and transparent for stained cells to be visible from the surface (Meilhac et al., 2004; Tzouanacou et al., 2009; Sequeira and Nicolas, 2012). Although this is the case for the livers of E11.5 and E12.5 embryos, by the time the livers have reached E13.5 the hematopoietic contribution renders the tissue dense, and this certainly results in a significant underestimation of cluster numbers because counts only include cells visible from the surface. We sectioned livers from E16.5 embryos to compare the cluster numbers and sizes within the lobes with those on the surface. The sizes and numbers of clusters were similar for the inner parts of the lobes and for the surface (Fig. S2; χ^2 test, P=0.09). The total liver volume is ~2.8 times greater than the volume visible from the surface (assuming a depth of view of 250 µm). We therefore have only sampled ~36% of the total volume, but clusters show similar distributions within the tissue and on the surface.

Time of emergence of the stained clusters

Our large collection of embryos should permit us to calculate the probable dates of emergence of clusters in the embryos of different ages. To do so, it is crucial to correct for any differences in cell division rates. The mammalian embryonic liver is heavily populated by hematopoietic cells. A publication from 1969 (Paul et al., 1969) provides daily counts with a breakdown of the cells in the mouse liver from E12.5 to E18.5 with enumeration of the blood cells and hepatoblasts/hepatocytes. This provides the basis for correction of cell division rate differences. Fig. 5A gives the calculated generation times for hepatoblasts/hepatocytes between E11.5 and E16.5 (the growth curves are shown in Fig. S3). Fig. 5B shows, for each embryonic day (E-day) examined, the numbers of clones as bars that are colored to show the numbers of cell divisions accomplished. The calculated E-day of emergence of each group of clusters can be read directly from the E-day scale shown at the bottom of the figure.

It can be seen that the majority of clusters in the E15.5-E16.5 collections emerged between E11.5 and E13.5. Irrespective of the age of the embryos, the majority of clusters have undergone three to six divisions, indicating that this could represent a limit to their embryonic growth behavior. Very few have undergone more than eight or nine divisions. Although it appears that E13.5 embryos contain more of the larger (more than six divisions) clusters, on a proportional basis this is not the case (Table 1). As regards the time of emergence, there appear to be two phases: progenitor cells generated between E8.5 and E11.5, and a second group between E11.5 and E13.5, the later time corresponding to the end of the phase of rapid hepatoblast/hepatocyte growth.

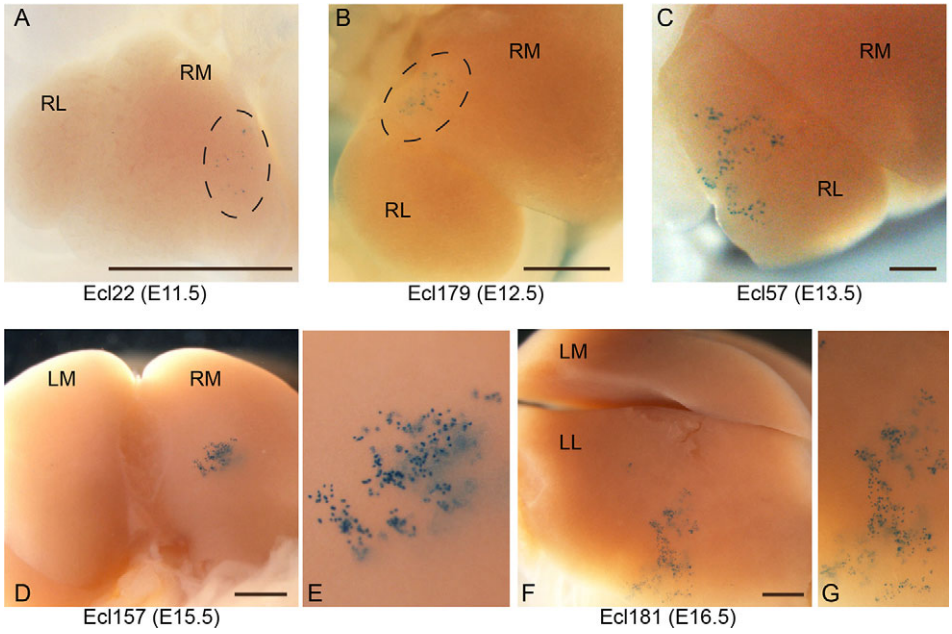

Fig. 2. Clusters of stained cells in E11.5 to E16.5 embryos. (A-G) Photos of representative clusters of cells stained with X-gal reagent in livers of E11.5 to E16.5 embryos. One image per age examined is given; other examples are shown in Fig. S1. A-C show images of embryos lying on the left side, with the right side facing the camera; D (enlarged 5× in E) shows the rostral view from the posterior; F shows the deep LL (which appears flattened at older ages) photographed from the ventral side (enlarged 2× in G). (A) Ecl 22 (E11.5): the photograph shows the large RM with the smaller RL to the left. The liver is still nearly transparent; 21 blue nuclei are located in the RM lobe: a dashed oval surrounds the area. At this stage, *Hnf4a* is weakly expressed, so the blue nuclei are pale. (B) Ecl 179 (E13.5) presents 46 cells positioned (inside dashed oval) on the lower edge of the RM. (C) Ecl 57 (E13.5) is situated on the still small RL, and the distribution of the 160 cells is suggestive of stripes. (D,E) The labeled cells of Ecl 157 (302 cells; E15.5) lie only partially on the surface of the RM; shadows of more deeply lying cells are visible. (F,G) The cells of Ecl 181 (E16.5) are widely distributed within an area of the LL. This cluster (450 cells) might be an early manifestation of what could become a broad stripe. Scale bars: 500 µm. LL, left lateral lobe; LM, left medial lobe; RL, right lateral lobe; RM, right medial lobe.

Development (2016) 143, 1149-1159 doi:10.1242/dev.132886

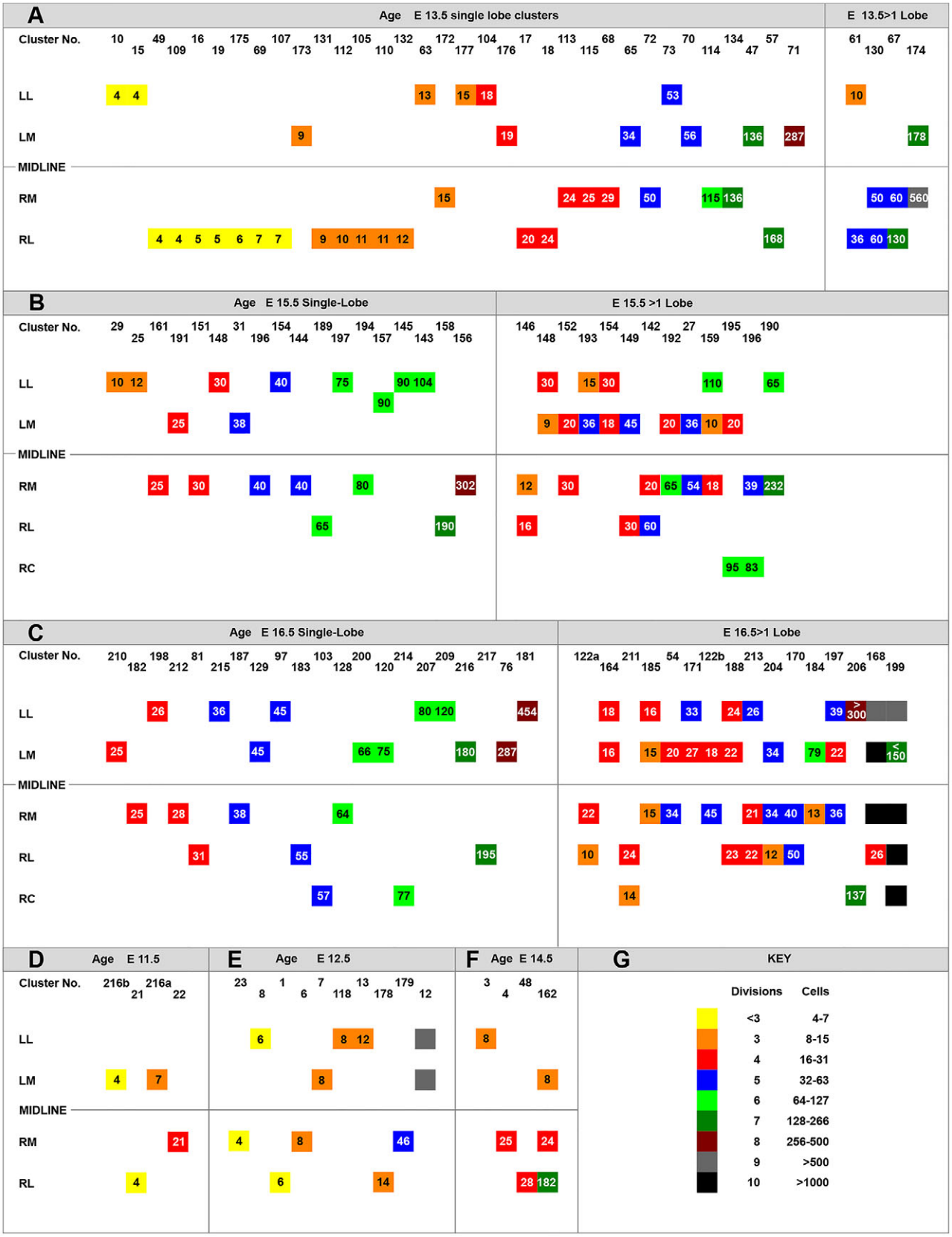

Fig. 3. Summary schemes illustrating the characteristics of clusters in the livers of E11.5 to E16.5 embryos. (A-F) Each panel follows the same pattern. At the top is the age group and just underneath is the cluster (or liver) identifying number. Below are represented the different lobes, arranged as seen from a rostral view. The midline is situated between the LM and the RM. The vertical position of the boxes indicates the lobe(s) in which the cluster was observed, the number within the box gives the number of cells counted, the color of the box indicates the estimated number of generations required to form a cluster of that size. (G) Key for box colors. LL, left lateral lobe; LM, left medial lobe; RC, right caudate lobe; RL, right lateral lobe; RM, right medial lobe.

Development (2016) 143, 1149-1159 doi:10.1242/dev.132886

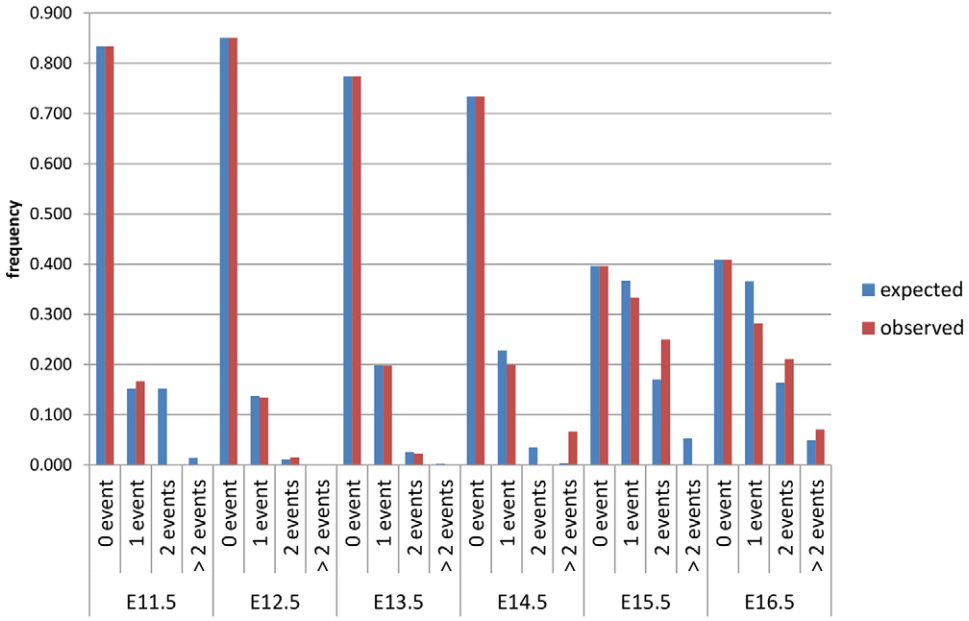

Fig. 4. Comparison of the expected and observed frequencies of recombination events at successive developmental stages. The Luria–Delbrück fluctuation test indicates that clusters in different lobes mostly result from independent events. The observed frequencies report the number of different lobes containing blue cells in one embryo with 1, 2 and >2 events representing clusters in one, two or more than two lobes. The expected frequencies were computed assuming that each recombination is a spontaneous random event, and estimating the λ parameter of the Poisson distribution from the proportion P of negative embryos [P=exp(−λ)]. The observed values (red) correspond almost exactly to the expected values (blue) and for each developmental stage the two distributions are not statistically different [χ^2 test, with Yates's correction, P>0.68; n=24 (E11.5), 67 (E12.5), 177 (13.5), 15 (14.5), 48 (15.5) and 71 (16.5)]. Therefore, it may be concluded that the majority of embryos have undergone independent events when two or more lobes contain blue cells. However, as discussed in the text, considerations of proximity of the labeled lobes and of the distributions of cells within the lobes led us to propose that some of the multi-lobe clusters are the result of a single recombination event, i.e. they are clones.

Cluster patterns in postnatal livers: spots, stripes and broad stripes

Young transgenic mice were analyzed at 3 to 5 weeks of age to determine the evolution of clusters of blue cells. Many were indeed observed, but on a background of numerous very small clusters (<15-20 cells). We have followed only those of significant size in order to define patterns of cell distribution, and these larger clusters were observed in 34% of the 141 animals examined. This frequency falls within the ranges of those observed in the embryo, as would be expected from the dramatic reduction in growth rates of liver cells in older embryos and young mice.

The distribution of cells within clusters describes two distinct forms: spots and stripes. Unlike the embryonic clusters, those from the young mice were composed of very closely associated cells that are most often too closely apposed to permit cell counts. This is due to tight adherence of the cells to one another, the strong expression of *Hnf4a* in postnatal hepatocytes, and the cessation of hematopoiesis in the liver.

Both spots and stripes reveal that daughter cells remain close to their parents. A stripe would result if cells show oriented division or intercalation or migration combined with oriented adherence, whereas daughters clustered among themselves as well as with their parents in a radial fashion would form spots (Fig. 6A,B).

The spot clusters occur most frequently in groups, giving rise to patterns of spots reflecting a combination of dispersed and cohesive growth. The most common patterns are alignments, giving rise to stripes composed of multiple spots, and wandering spots where the arrangement is apparently random within a limited territory. Spot clusters give the impression that all are from a single progenitor cell with progeny that were more mobile around the time when the clone was initiated (dispersed growth) than when most of the growth occurred (cohesive growth). Examples of aligned spots and wandering spots are shown in Fig. 6C-F. The spots and stripes both reveal properties anticipated of hepatocytes: close association among the cells as exemplified by expression in the mature cell of a variety of cell adhesion molecules (Battle et al., 2006).

Liver AH (see Materials and Methods for explanation of terminology) (Fig. 6G,H) shows a striking pattern: the left lateral lobe, on both the rostral and the caudal sides, has two very clear broad radial stripes. This is not the only example of broad radial stripes in the left lateral lobe: they can also be seen in Figs 7 and 8: in liver AI (Fig. 7C,D) visible on both the rostral and caudal sides, in liver BC (Fig. 7E,F) and in Ecl 168 (Fig. 8A,B), as well as in Ecl 181 (Fig. 2F). Considering all of the images of the left lateral lobe, two to three broad stripes are clear on the anterior part of the lobe and five to six on the lateral and posterior sides, giving the impression that seven to nine broad stripes have been visualized, with possibly an equal number that were not picked up in our analysis. We suggest that at least nine and perhaps ∼20 cells, each giving rise to a broad stripe, underlie the morphogenesis of this lobe, the largest of the liver lobes in the mouse. Early signs of broad stripes are also present in the right lateral lobe of Ecl 57 (Fig. 2C). Although most of these examples of broad radial stripes do show blue shadows indicative of deeply embedded stained cells, serial sections would be required to affirm that they traverse the entire lobe.

Mega-clones: multi-potentiality and acquisition of left-right identity

As the Luria–Delbrück test (Fig. 4) has shown that all of the embryonic clusters, including the multi-lobe ones, could result from independent events, how do we decide which are clones? The major criteria include labeled cells in more than one tissue, as well as

Development (2016) 143, 1149-1159 doi:10.1242/dev.132886

A

embryonic day intervals	11.5 - 12.5	12.5 - 13.5	13.5 - 14.5	14.5 - 15.5	15.5 - 16.5	16.5 - 17.5
generation time in hours	12	12.6	18	20.9	>48	>48

B

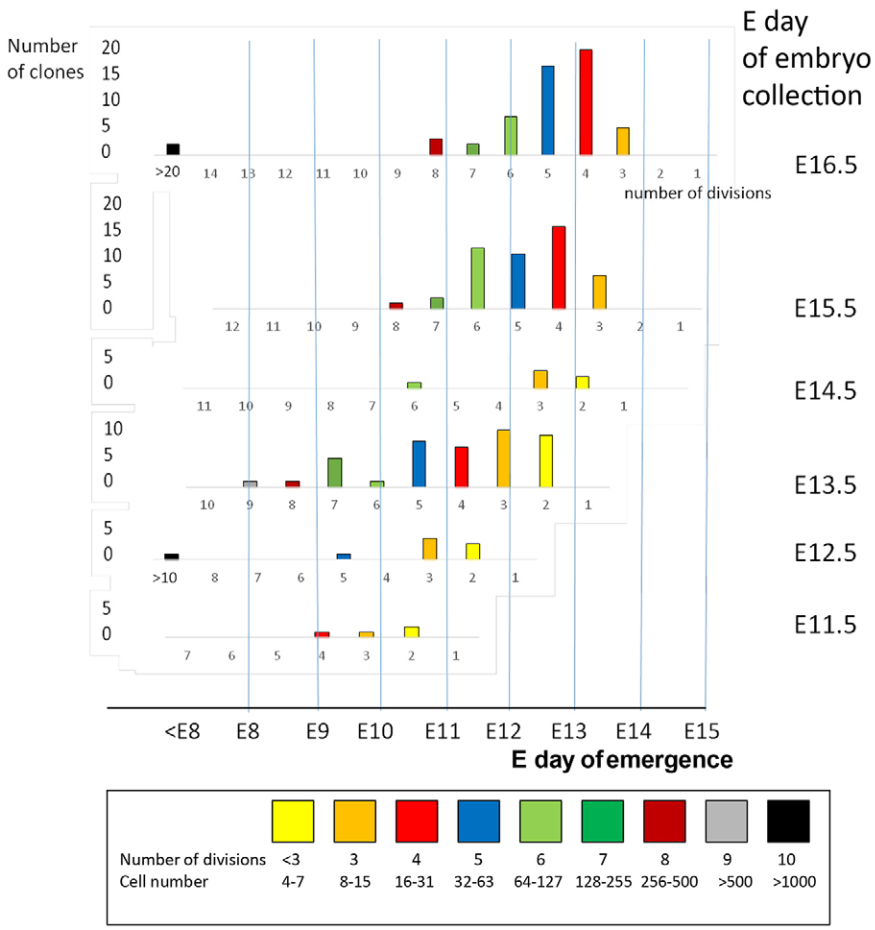

Fig. 5. Predicted time of emergence of embryonic clusters: a retrospective analysis. (A) Calculated cell generation times from the data of Paul et al. (1969). (B) Graphic placement of cluster size groups on the embryonic day (E-day) corresponding to the number of cell generations that have taken place, and corrected for the shifts caused by the shorter or longer generation times. The number of cell divisions is indicated below each age group of histograms. The colors shown at the bottom of the figure correspond to the numbers of cell divisions as in Fig. 3. All clusters that emerged prior to E8 have been regrouped as <E8.

numbers and density of stained cells and their location within and between lobes. Two very large clones in a single embryo are improbable, especially if the lobes involved are contiguous. From our collection of 402 embryos we have recovered four that we refer to as mega-clones: two of the multi-lobe clusters of the E12.5-E13.5 embryos, Ecl 12 and 130, and from two older E16.5 embryos, Ecl 168 and 199, which are particularly interesting because all of the lobes are populated by blue cells, indicating that the event underlying their origin occurred very early in development. From the 141 postnatal mice, we have obtained four mega-clones. This is a total of eight livers carrying mega-clones, out of 543 specimens, corresponding to a frequency of 0.015. (The probability of having two equally large clones in the same liver is of the order of 0.0002.) From these mega-clones we can draw a number of conclusions concerning composition and morphogenesis of the endoderm and, in particular, of the liver. The mega-clones are presented below beginning with the highest densities and widest distributions of marked cells. Table 2 summarizes their properties.

The first mega-clone is designated AT: the liver is entirely stained, as is the pancreas (Fig. 7A,B). The only unstained cells in the pancreas are fat cells (not informative because adipose cells do not express *Hnf4a*). The clone originated from a precursor cell that contributed (at least) to the dorsal and ventral pancreas as well as the liver, or possibly from a progenitor from an even earlier stage. Only the pancreas and liver from the mouse were examined, so the possibility that the progenitor cell arose among the earliest definitive endoderm cells cannot be excluded. Indeed, it could even have arisen before delineation of the endoderm, but only sequencing of the reporter could provide information because *lacZ* expression is under control of the *Hnf4a* gene.

The AI liver (Fig. 7C,D) and Ecl 168 (Fig. 8A,B) both contain blue cells in all lobes of the liver and several regions of blue acini are present in the part of the pancreas derived from the dorsal pancreatic bud; Ecl 168 also shows stained cells in the intestine. These three mega-clones are of the same class: multi-potent (for more information on clusters in tissues other than the liver, see Fig. S4).

Ecl 199 (Fig. 8C,D) has stained cells in all lobes of the liver but none in the pancreas; however, it also has labeled cells in the intestine. There is an intense concentration of blue cells in the caudate lobe, much more so than in the right lateral lobe from which

Development (2016) 143, 1149-1159 doi:10.1242/dev.132886

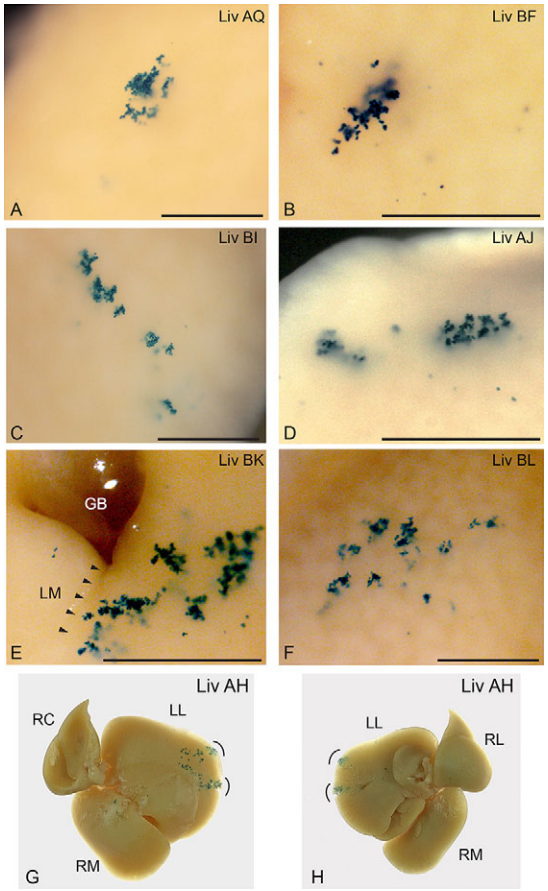

Fig. 6. Cluster patterns in livers of postnatal 3- to 5-week-old mice: spots and stripes. (A) Liver (Liv) AQ, a central group of stained cells is surrounded by three smaller groups. (B) A stripe on Liv BF, with some cells radiating out laterally to make a figure resembling a zipper. (C) Liv BI exhibits six spots, mostly aligned. (D) Liv AJ shows lines of star-like dense spots. (E) Liv BK, where five or six irregular dense spots are found on the RM, aligned at the midline just beneath and to the right of the glistening gall bladder (GB). Note that cells do not appear to cross the midline to converge on the LM (arrowheads). (F) Liv BL exhibits irregular dense spots. (G,H) Photographs of the rostral and caudal views, respectively, of Liv AH show large groups of stained cells visible only in one lobe, the LL, where two clear broad stripes can be seen on the lateral portion (curved lines) of both the rostral (left) and caudal surfaces. Scale bars: 500 µm. LL, left lateral lobe; LM, left medial lobe; RC, right caudate lobe; RL, right lateral lobe; RM, right medial lobe.

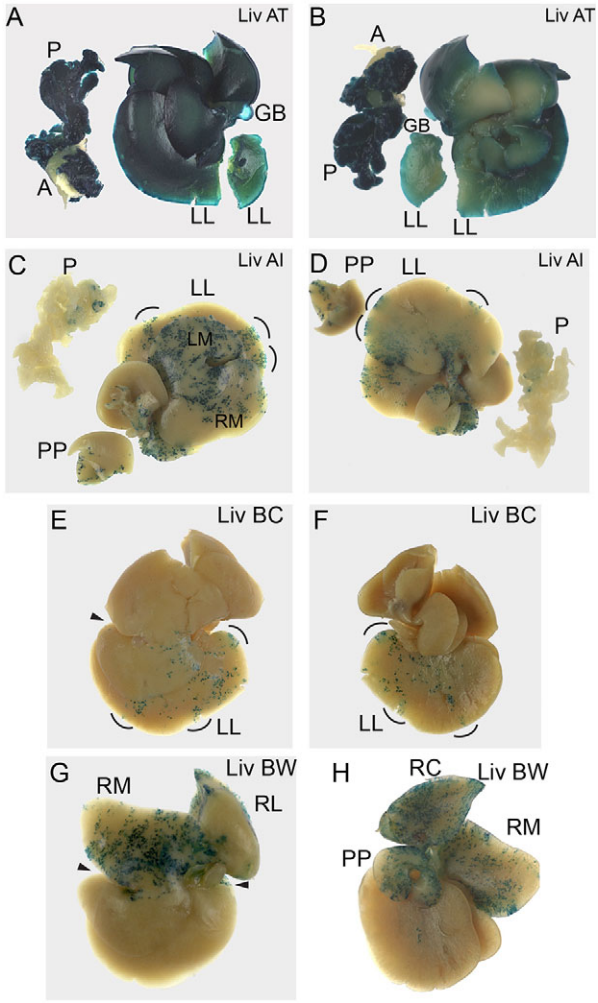

Fig. 7. Mega-clones of livers from postnatal 3- to 5-week-old mice. Note that the right small (RL and RC) lobes are sometimes twisted back from the body of the liver and appear outside of the oval outline of the liver. Specimens are shown from both the rostral (left) and caudal (right) views. Curved lines indicate positions of broad stripes. (A,B) Liver (Liv) AT with strongly labeled cells throughout the liver and pancreas (P, on the left). The anterior part of the LL is broken off and is placed next to the lobe. Staining of the caudal side of the liver is less blue owing to incomplete diffusion of the X-gal substrate. The white areas of the pancreas are adipose (A) tissue. The pale shiny protrusion is the gall bladder (GB). (C,D) Rostral view (C) of Liv AI shows that both the LM and RM lobes have many labeled cells that cover much of the rostral surface of the liver. The caudal view (D) shows less labeling, although all lobes contain blue cells. Part of a papillary process (PP) has been broken off and is placed near to the liver. The pancreas, the irregular body to the left (C) or the right (D) of the liver, also contains some marked areas. (E,F) Liv BC is an example of a 'left-only' label: from the rostral view (E) it can be seen that a line demarcates the stained region, just to the right of the midline (arrowhead). Note that none of the small lobes of the right side of the liver is marked. (G,H) Liv BW is a 'right-only' liver: again, from the rostral view (G) a demarcation line can be discerned (arrowheads). The caudal (H) doughnut-shaped PP is intact, and the RL lies on top of the RC. LL, left lateral lobe; LM, left medial lobe; RC, right caudate lobe; RL, right lateral lobe; RM, right medial lobe.

it emerged. This implies that a group of cells destined to make the caudate lobe was set aside, either early during formation of the right lateral lobe or of the liver itself, before the blue cells of the right lateral lobe were diluted by growth of unlabeled cells.

Liver BC (Fig. 7E,F) and Ecl 12 (Fig. 8E,F) have numerous stained cells but only on the left side. The rostral view of liver BC shows a clear line of cells that separate the two halves of the liver. Ecl 12 is a particularly informative clone because >1000 cells can be counted, revealing that at least ten generations have been accomplished in this embryo at only 12.5 days of development. Had this mega-clone been detected in an older embryo or a neonate, even more stained cells would have been present. Referring to the scale of Fig. 5B, we can place emergence of this clone sometime before E8.

Liver BW (Fig. 7G,H) shows intense staining in all cells of the right side of the liver with a particularly clear line separating the right from the left on the rostral side. The labeling of the caudal view (Fig. 7H) indicates that the small lobes belong to the right side of the liver. Ecl 130 (E13.5) shows the same cell distribution: right side only with stained cells in all right lobes, including the partially formed caudate lobe and the future papillary process (not shown). These two clones are of the same 'right-only' class.

These eight clones inform us of the properties of multi-potential precursors that contribute to both the liver and the pancreas: the cells are competent to occupy all spaces of the liver

Development (2016) 143, 1149-1159 doi:10.1242/dev.132886

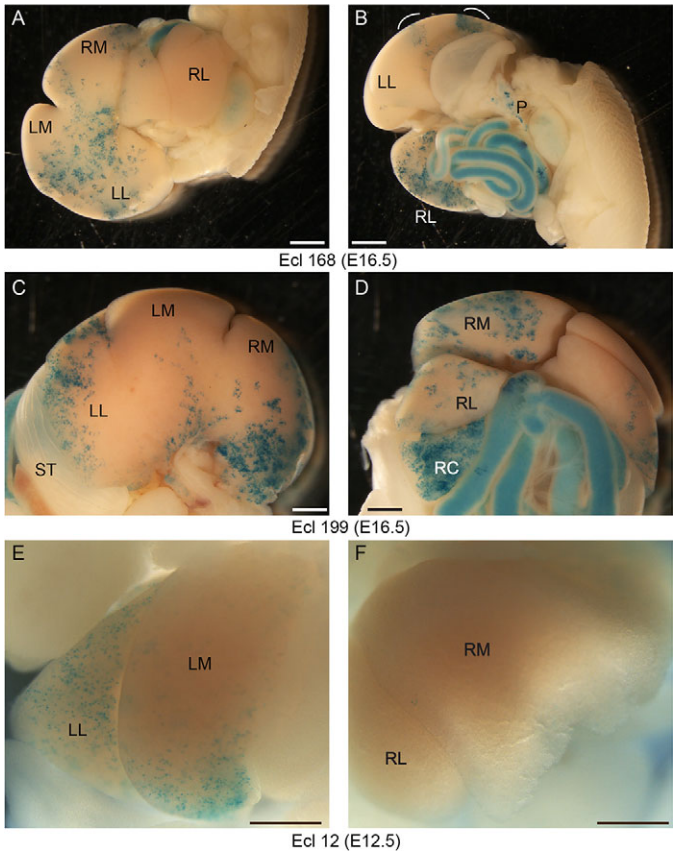

Fig. 8. Mega-clones from embryos. (A,B) Rostral and visceral views of E16.5 Ecl 168. The LM and LL are well marked, as is the visceral side of the RL. All lobes contain stained cells. Note clusters of blue cells in the pancreas (P). The looped intestine contains pale blue material, which appears beginning at ~E15.5 (results not shown). Very dark spots that are clones can be clearly distinguished from the background thanks to the nuclear localization of the β-gal staining. (C,D) Rostro-posterior and antero-ventral views of E16.5 Ecl 199. This embryo shows preferential marking on the right side, but blue cells are present in all lobes. The RC lobe is much more densely populated with blue cells (D) than the RL (just above) from which it emerged 2 days before. Next to the RL a strong staining can be seen on the gut tube just where it loops back. (E,F) Ecl 12, a left-sided clone from an E12.5 embryo: E, viewed from the left side of the embryo, F, the right side view. The blue cells are widely distributed in the LM and LL; >1000 cells can be counted. On the right side, a few scattered blue cells can be observed (not visible here). LL, left lateral lobe; LM, left medial lobe; RC, right caudate lobe; RL, right lateral lobe; RM, right medial lobe.

and clearly have enormous growth potential. Only one clone occupies all of the liver lobes and does not contribute to the pancreas: this is Ecl 199, from an E16.5 embryo. Although the similarly aged Ecl 168 does show extensive participation in pancreas development, expression of *Hnf4a* occurs only at mid-gestation in this tissue, so a slight lag in onset of expression could be responsible for the absence of marked cells in the pancreas of Ecl 199.

The frequency of appearance of pancreas and liver clusters implies that the progenitor cell pool for the pancreas is many times smaller than that for the liver. Among the 402 embryos, only one contained pancreas clusters. However, because *Hnf4a* expression in the pancreas occurs only at mid-gestation, we can compare frequencies only for the 129 E15.5 and E16.5 embryos. Among them, 99 probably independent liver clusters were observed, but only one contained labeled cells in the pancreas, implying a 100-fold difference in the progenitor pools for the two tissues (pancreas clusters were also observed in two neonatal mice that did not contain liver clusters). These results complement and confirm those of Tremblay and Zaret (2005) and Stanger et al. (2007).

Sometime soon after loss of bi-potentiality, liver cells become restricted to growth on only one side of the liver: left or right. This was an entirely unexpected finding. Interestingly, our collection contains one embryonic and one postnatal example of each exclusive occupation, left or right.

DISCUSSION

This analysis has provided information on the growth patterns of the liver, the existence of multi-potent cells within the embryonic endoderm and a left-right chirality decision in the liver that most likely occurs after restriction of cells to the liver fate. It shows as well the oriented and cohesive behavior of hepatoblasts/hepatocytes forming clusters rather than a generalized dispersion within the tissue, and the morphogenesis of the largest of the lobes, the left lateral, implicating broad stripes formed from a small number of precursors. In addition, this work provides evidence that clones of liver cells emerge not at a constant rate during early embryogenesis, but mainly during the phases of rapid expansion of the tissue, after E8.5 and until E13.5. Finally, the distribution of sizes of the vast majority of clusters/clones indicates that the tissue is formed not by stem cells, but by symmetrical divisions of somatic hepatoblasts/hepatocytes, with the exception of the progenitors of mega-clones, which have descendants in the intestine and pancreas as well.

The density of stained cells in the mega-clone embryos indicates that many thousand, and perhaps millions, of descendants are present, implying that at least 20 cell generations have elapsed. For the tiny group of eight mega-clones among the 543 specimens, the number of divisions per clone far exceeds those of the three to eight division clusters observed in nearly all of the embryos, as depicted in Figs 3 and 5. We conclude that these mega-clones constitute a separate class. Clearly, there is a gap of more than ten generations in the growth shown by the majority of clones and those designated as mega-clones, and the existence of this gap indicates that at least two classes of progenitor cells participate in formation of the liver. Fig. 9 depicts as histograms the numbers of clusters having undergone between three and nine divisions, drawn from the data of all embryonic ages examined. This distribution coincides closely with the signature pattern for clones of somatic cells: an exponential decrease is observed in the numbers of larger clusters. This is the pattern expected from symmetrical growth of somatic cells with a limited number of divisions. By contrast, the mega-clones fall into a different class, characterized by the enormous growth potential expected of the earliest endoderm cells (or stem cells; see Nicolas et al., 1996 and Meilhac et al., 2003 for further discussion of the subject). However, our transgene was designed to be expressed only in certain endoderm derivatives, so we cannot comment on other cell types. Compellingly, several of the mega-clones are derived from progenitors with multi-potentiality, a common characteristic of very early embryonic cell populations.

The left-right decision is likely to occur soon after restriction of progenitors to a liver-only fate. For example, comparison of mega-clones AI and BW show comparable density of marked cells, but AI descendants occupy all lobes plus the pancreas, whereas BW is a right-only liver clone. The liver is clearly an asymmetrical organ among several in the viscera, but it has not been clear whether its asymmetry is a consequence of that of the major blood vessels around which it forms (Meno et al., 1998; Hamada et al., 2002). The

Development (2016) 143, 1149-1159 doi:10.1242/dev.132886

Table 2. Properties of mega-clones

		Liver lobes				Late-appearing lobes		
Class	Identity	LL	LM	RM	RL	RC	PP	Pancreas
Multi-potent	AT	+++++	+++++	+++++	+++++	+++++	+++++	+++++
Bi-potent	AI	++	+++	++	+	+	++	+
Multi-potent	Ecl 168	++	+++	+++	+	+	?	++
Bi-potent	Ecl 199	++	+	+++	++	++++	?	0
Left only	BC	+++	++	0	0	0	0	0
Left only	Ecl 12	+++	+++	0	0	–	–	–
Right only	BW	0	0	++++	++	+++	+	0
Right only	Ecl 130	0	0	++	++	–	–	–

LL, left lateral lobe; LM, left medial lobe; PP, papillary process; RC, right caudate lobe; RL, right lateral lobe; RM, right medial lobe.
Intensity of labeling: +++++, all cells labeled; ++++, most cells labeled; +++, many cells labelled; ++, few cells labelled; +, labelled cells rare; 0, no cells labeled; –, an answer cannot be provided because: the tissue was not conserved, the transgene would not yet be expressed due to late onset of *Hnf4a* expression in the embryonic tissue, or the late-appearing lobe was absent; ?, tissue was lost or was not visible.

existence of left-side only and right-side only clones reveals a cellular basis for chirality of the liver.

A fundamental question that can be addressed by clonal analysis is how a given organ develops. The mammalian liver is formed mainly by cells of the hepatic diverticulum, an outgrowth of tissue on the ventral side of the foregut that invades the STM. A number of autonomously acting genes as well as growth factors from the mesenchymal environment stimulate the endodermal cells to migrate, delaminate into the STM and proliferate rapidly for 48-72 h before the liver emerges from the STM at E11.5 (references in the Introduction). Surprisingly, the entire liver capsule can be formed by the mesenchymal elements of the liver (Sosa-Pineda et al., 2000).

We now know that hepatocytes do not simply flow into and fill the liver by successive cell divisions: they acquire a side-limited identity, proliferating on the left or the right side. In addition, they form fields of cells with defined identity that appear to be set aside to play a specific role in development. For example, at E12.5 the embryo exhibits no sign of the small right lobes. The tissues that will form these lobes emerge from the right lateral lobe as thickened sheets that grow into lobes within two days. In the E16.5 embryo of Ecl 199, the right caudate lobe is densely packed with blue cells that must have arisen from the weakly marked right lateral lobe (Fig. 8C). This discrepancy clearly implies that a densely marked group of cells was set aside early in the formation of the right lateral lobe, to participate at a later date in morphogenesis of the right caudate lobe. Furthermore, the morphogenesis of the largest lobe, the left lateral, appears to occur via the proliferation of a small group of progenitor cells, which we would estimate to number around nine based upon the positions of the broad stripes observed. The mega-clone AH illustrates two broad radial stripes or spokes that appear to radiate outwards from a central point of the left lateral lobe. Similar broad radial stripes in the left lateral lobe are also visible in five other livers, mentioned in the Results. The existence of broad radial stripes strongly implies that oriented growth occurs in the formation of liver lobes.

Now, we focus on the clusters/clones of small to intermediate size that constitute the majority of the collection. The forms of these clusters are very much what one would have predicted from what is known about the behavior of liver cells in culture, and their differentiation during development. During the early phases of liver development (E11.5 to E13.5), the epithelial cells are not closely apposed to one another, being well dispersed among the mesenchymal cells (Vassy et al., 1988). As development proceeds, the hepatoblasts/hepatocytes begin to fill the liver in a more dense fashion, forming liver cell cords, as blood vessels emerge from the earlier sinusoid spaces. In the liver after birth, the hepatocytes are highly polarized and packed against one another in brick-like fashion, held in place by numerous intercellular junctions. Thus, clusters from 3-week-old liver are tightly packed, those from around E15.5 begin to show associations in groups of cells clustered together, and the clusters from earlier embryos are only loosely associated.

Finally, the retrospective calculation of emergence time of the intermediate sized clusters has permitted us to estimate that the most rapid growth phase of the liver occurs early, with a relatively

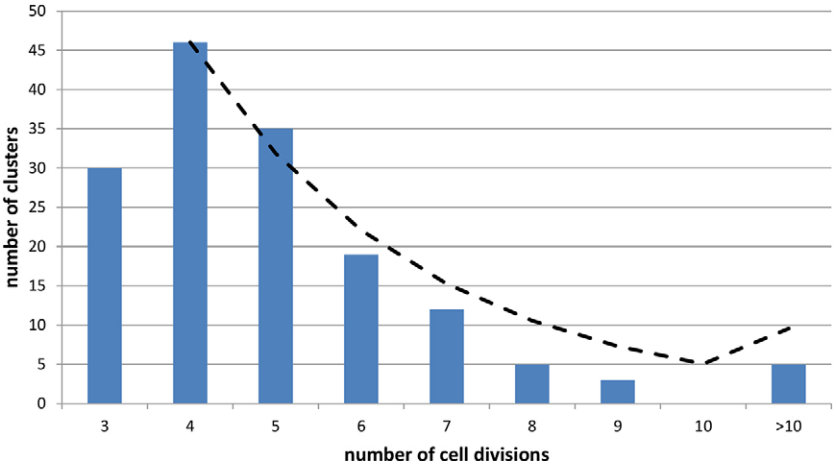

Fig. 9. Relationship between cluster size (deduced from numbers of cell divisions) and their frequency. Cumulative numbers are given from all embryonic ages of clusters. After the peak at four divisions there is an exponential decline in the frequencies of larger clusters, characteristic of a somatic cell symmetrical growth mode. The form of the graph gives no indication of departure from a normal size/frequency distribution (dashed line), as would be expected if significant numbers of cells had left the hepatoblast/hepatocyte differentiation pathway to join an HNF4α-negative one (for example, the intra-hepatic biliary system). The dashed line is the theoretical probability distribution of the corresponding exponential distribution. The two distributions are not significantly different (Kolmogorov–Smirnov test, P=0.7).

Development (2016) 143, 1149-1159 doi:10.1242/dev.132886

high frequency of clusters being born prior to E11, when the prospective liver is still in the STM. For example, the very rapid growth rates at E9.5 can be deduced from the data of Bort et al. (2006) who found by labeling of phosphorylated histone H3 that half of the cells in the delaminating hepatic bud were in a mitotic phase. The clusters of our early embryos seem to have been born mainly between E8.5 and E11.5 and those of the later embryos mainly from E11.5 to E13.5. After this later time, Paul et al. (1969) have determined that growth rates decline significantly, as does the generation of clusters of labeled cells.

Do the results reported here contribute to the long-term discussion concerning the plasticity of differentiation of liver cells from adult animals and the possible existence of liver stem cells? It is important in this context to underline the fundamentally different nature of the experiments: the results on liver cells from adults, whether in liver regeneration experiments or *in vitro* growth conditions, concern manipulations to reveal growth/differentiation potential, whereas our lineage analysis was carried out on animals in the absence of experimental intervention, telling us what cells do when they are not stressed. We conclude from our analysis that the overwhelming majority of liver cells in the embryo show a limited potential to proliferate *in situ* during normal development, although the growth potential could change significantly upon stress. The progenitor cells that show huge growth potential, as observed in mega-clones, are rare and often associated with the multi-potential state so they might be limited to the early embryo. Adult life poses stresses, including time, that do not occur in the embryo, and such stresses provoke responses that would not be seen in their absence.

MATERIALS AND METHODS

Construction of the transgene, introduction of the knock-in allele, and generation of mice

The allele carrying *nLaacZ* sequences was constructed by recombineering and introduced into the mouse genome by the European Molecular Biology Laboratories (EMBL) Transgenic Facility (Monterotondo, Italy). The *nLaacZ1.1* clone contains nuclear localization sequences (n) upstream of the bacterial sequences coding for *Escherichia coli* β-galactosidase, into which a *Cla*I-*Sac*I intragenic duplication introduces a STOP codon (Meilhac et al., 2003). A viral IRES sequence, provided by Fred Relaix (Relaix et al., 2003), was placed upstream of *nLaacZ* and these elements were introduced into a BAC clone of the *Hnf4a* gene, at the *Sph*I site, 100 bp from the beginning of the 3′UTR sequences (see diagram in Fig. 1A). The vector was transfected into BRUCE4 embryonic stem cells (ESCs), and correctly recombined alleles were identified by sequencing. The recombined ESCs were injected into mouse blastocysts and five founder mice were obtained at the EMBL Transgenic Facility. One was bred with C57Bl6J×DBA mice. F1 mice were crossed with PGK-Cre mice (Lallemand et al., 1998) to remove the loxP-flanked *neo* cassette. The mouse colony was maintained as an outbred population. Sperm from the transgenic mice were frozen in the Institut Pasteur Animalerie Centrale Collection (Paris, France) [Ki HNF4α(3′UTR)$^{IRESnlaacZ1.1/+}$] and are available upon request.

Breeding of mice for analysis

Animal care was in accordance with institutional and national guidelines. Embryos up to E13.5 were obtained by crossing super-ovulated female B6SJL mice with homozygous transgenic males; for older embryos, super-ovulation was not used.

Removal of embryos, cleaning of tissues, fixation, X-gal staining and microscopy

Embryos were recovered from pregnant females into PBS. For E11.5 to E13.5 embryos, the abdominal wall was dissected away, leaving the viscera exposed. For older embryos, the abdominal wall was removed: the trunk was severed above the diaphragm and the diaphragm removed to expose the rostral surface of the liver. For postnatal mice, following cervical dislocation, the liver and pancreas were dissected out. The specimens/tissues for study were fixed in 4% paraformaldehyde for 30 min to 1 h, rinsed several times in PBS and stained overnight in X-gal solution (Tajbakhsh et al., 1996; for embryos of E15.5 and older, the concentration of NP40 was increased by a factor of three to enhance transparency). Embryonic clones were easy to count because the nuclei were not packed too tightly, and a reasonable degree of transparency permitted visualization of several layers of cells below the surface. The photographs have a more shallow depth of field than the microscope. Only clusters of four or more cells were counted (except in sections) because in whole mounts very small cell groups are easy to overlook. From E15.5, counts began with eight-cell clusters.

To obtain counts and characteristics of clusters within the tissue, fixed livers of 30 E16.5 embryos were conserved in cold PBS, then embedded in 2% agarose and sectioned at 200 µm using a Tissue Chopper (MacIlwain, Redding, CA, USA). Seven to ten sections were collected in each well of 24-well dishes (Falcon) in PBS, and treated as floating sections. The liquid was aspirated and replaced with X-gal staining solution overnight at 37°C. After staining, the solution was replaced with 4% paraformaldehyde. Sections were counted directly in the 24-well plates. Using this method, each well contained sections from multiple lobes, so it was not possible to establish continuity within clusters. Specimens were examined using a Leica MZ APO stereomicroscope.

Generation times from the literature of hepatoblasts/hepatocytes in the developing rodent liver

Two publications from the literature, Paul et al. (1969) and Vassy et al. (1988) have been used to estimate hepatoblast/hepatocyte generation times in the developing liver (see Fig. S3 for details).

Examination of embryonic tissues for β-gal-positive cells

Hnf4a, the mouse gene controlling expression of the transgene, is expressed from E8.5 in the hepatic diverticulum. In other tissues, it is expressed only from mid-gestation. Positive cells in the pancreas were observed in only one embryo, at E16.5. β-Gal-positive cells were frequently seen in the intestine of E15.5 and E16.5 embryos, but with an unexpected distribution: in a given litter, either intestinal clusters were observed in several embryos, or in none. This led us to conclude that the onset of *Hnf4a* expression in the intestine is variable during normal development. Therefore, we have not included intestinal clones in the results except as an argument for multi-potentiality when they were observed in mega-clones.

Statistical analysis

The clonality of labeling in embryos in which two or more lobes contain blue cells was assessed using the Luria–Delbrück fluctuation test (Luria and Delbrück, 1943) as detailed in the legend to Fig. 4.

Distributions were compared using a χ^2 test, with Yates's correction.

Terminology of stained cell clusters in embryos and young mice

Each cluster of β-gal$^+$ cells was assigned a number and designated Ecl (for embryonic cluster) followed by the cluster number. When more than one cluster was observed in an embryo, only the lowest cluster number is given (Fig. 3). For postnatal 3- to 5-week-old mice, each liver with at least one large cluster was given a two-letter name, e.g. AT.

Acknowledgements

We are grateful for the collaboration of Sigolène Meilhac and Didier Rocancourt in the initial stages of this project. Discussions with Ken Zaret, Jean-Francois Nicolas, Ana Cumano, Didier Montarras and Francesca Spagnoli are appreciated. We thank Jean-Marc Panaud and Richard Buckingham for valuable assistance. Dina Kremsdorf and the INSERM generously provided space to M.C.W. We thank the EMBL Transgenic Facility for preparing the recombinant mice.

Competing interests

The authors declare no competing or financial interests.

Author contributions

M.C.W. and M.B. planned the experiments; S.C. performed the mouse husbandry; M.C.W. analyzed the mice; J.-F.L.G. carried out statistical analysis; H.S.-M. prepared photographic figures; M.C.W. wrote the manuscript with input from M.B., J-F.L.G. and H.S.-M.

Funding

This work was supported by the Centre National de la Recherche Scientifique; the Institut National de la Santé et de la Recherche Médicale; the Institut Pasteur; and the Agence Nationale de la Recherche (Laboratoire d'Excellence Revive, Investissement d'Avenir) [ANR-10-LABX-73 to H.S.-M.].

Supplementary information

Supplementary information available online at
http://dev.biologists.org/lookup/suppl/doi:10.1242/dev.132886/-/DC1

References

Battle, M. A., Konopka, G., Parviz, F., Gaggl, A. L., Yang, C., Sladek, F. M. and Duncan, S. A. (2006). Hepatoctye nuclear factor 4α orchestrates expression of cell adhesion proteins during the epithelial transformation of the developing liver. *Proc. Natl. Acad. Sci. USA* **103**, 8419-8424.

Bonnerot, C. and Nicolas, J. F. (1993). Clonal analysis in the intact embryo by intragenic homologus recombination. *C. R. Acad. Sci. III* **316**, 1207-1217.

Bort, R., Signore, M., Tremblay, K., Martinez Barbera, J. P. and Zaret, K. S. (2006). Hex homeobox gene controls the transition of the endoderm to a pseudostratified, cell emergent epithelium for liver bud development. *Dev. Biol.* **290**, 44-56.

Crawford, L. W., Foley, J. F. and Elmore, S. A. (2010). Histology atlas of the developing mouse hepatobiliary system with emphasis on embryonic days 9.5–18.5. *Toxicol. Pathol.* **38**, 872-906.

Duncan, S. A., Manova, K., Chen, W. S., Hoodless, P., Weinsein, D. C., Bachvarova, R. F. and Darnell, J. E. (1994). Expression of transcription factor HNF-4 in the extraembryonic endoderm, gut, and nephrogenic tissue of the developing mouse embryo: HNF-4 is a marker for primary endoderm in the implanting blastocyst. *Proc. Natl. Acad. Sci. USA* **91**, 7598-7602.

Duncan, S. A., Nagy, A. and Chen, W. (1997). Murine gastulation requires HNF-4 regulated gene expression in the visceral endoderm: tetraploid rescue of Hnf-4(-/-) embryos. *Development* **124**, 279-287.

Golub, R. and Cumano, A. (2013). Embryonic hematopoiesis. *Blood Cell. Mol. Dis.* **51**, 226-231.

Gualdi, R., Bossard, P., Zheng, M., Hamada, Y., Coleman, J. R. and Zaret, K. S. (1996). Hepatic specification of the gut endoderm in vitro: cell signaling and transcriptional control. *Genes Dev.* **10**, 1670-1682.

Hamada, H., Meno, C., Watanabe, D. and Saijoh, Y. (2002). Establishment of vertebrate left-right asymmetry. *Nat. Rev. Genet.* **3**, 103-113.

Hayhurst, G. P., Lee, Y.-H., Lambert, G., Ward, J. M. and Gonzalez, F. J. (2001). Hepatocyte nuclear factor 4alpha (nuclear receptor 2A1) is essential for maintenance of hepatic gene expression and lipid homeostasis. *Mol. Cell. Biol.* **21**, 1393-1403.

Hunter, M. P., Wilson, C. M., Jiang, X., Cong, R., Vasavada, H., Kaestner, K. H. and Bogue, C. W. (2007). The homeobox gene Hhex is essential for proper hepatoblast differentiation and bile duct morphogenesis. *Dev. Biol.* **308**, 355-367.

Jung, J., Zheng, M., Goldfarb, M. and Zaret, K. S. (1999). Initiation of mammalian liver development from endoderm by fibroblast growth factors. *Science* **284**, 1998-2003.

Kaufman, M. H. (1992). *The Atlas of Mouse Development*. San Diego, USA: Academic Press.

Kaufman, M. H. and Bard, J. B. L. (1999). *The Anatomical Basis of Mouse Development*. San Diego, USA: Academic Press.

Lallemand, Y., Luria, V., Haffner-Krausz, R. and Lonai, P. (1998). Maternally expressed PGK-Cre transgene as a tool for early and uniform activation of the Cre site-specific recombinase. *Transgenic Res.* **7**, 105-112.

Le Douarin, N. (1975). An experimental analysis of liver development. *Med. Biol.* **53**, 427-455.

Lee, C. S., Friedman, J. R., Fulmer, J. T. and Kaestner, K. H. (2005). The initiation of liver development is dependent on Foxa transcription factors. *Nature* **435**, 944-947.

Luria, S. and Delbrück, M. (1943). Mutations of bacteria from virus sensitivity to virus resistance. *Genetics* **28**, 491-511.

Martinez Barbera, J. P., Clements, M., Thomas, P., Rodriguez, T., Meloy, D., Kioussis, D. and Beddington, R. S. (2000). The homeobox gene hex is required in definitive endodermal tissues for normal forebrain, liver and thyroid formation. *Development* **127**, 2433-2445.

Meilhac, S. M., Kelly, R. G., Rocancourt, D., Eloy-Trinquet, S., Nicolas, J.-F. and Buckingham, M. E. (2003). A retrospective clonal analysis of the myocardium reveals two phases of clonal growth in the developing mouse heart. *Development* **130**, 3877-3889.

Meno, C., Shimono, A., Saijoh, Y., Yashiro, K., Mochida, K., Ohishi, S., Noji, S., Kondoh, H. and Hamada, H. (1998). Lefty-1 is required for left-right determination as a regulator of lefty-2 and nodal. *Cell* **94**, 287-297.

Nakhei, H., Lingott, A., Lemm, I. and Ryffel, G. U. (1998). An alternative splice variant of the tissue specific transcription factor HNF4alpha predominates in undifferentiated murine cell types. *Nucleic Acids Res.* **26**, 497-504.

Nicolas, J. F., Mathis, L., Bonnerot, C. and Saurin, W. (1996). Evidence in the mouse for sellf-renewing setm cells in the formation of a segmented longitudinal structure, the myotome. *Development* **122**, 2933-2946.

Paul, J., Conkie, D. and Freshney, R. I. (1969). Erythropoietic cell population changes during the hepatic phase of erythropoisis in the foetal mouse. *Cell Tissue Kin.* **2**, 283-294.

Relaix, F., Polimeni, M., Rocancourt, D., Ponzetto, C., Schäfer, B. W. and Buckingham, M. (2003). The transcriptional activator PAX3-FKHR rescues the defects of *Pax3* mutant mice but induces a myogenic gain-of-function phenotype with ligand-independent activation of Met signaling in vivo. *Genes Dev.* **17**, 2950-2965.

Rojas, A., De Val, S., Heidt, A. B., Xu, S.-M., Bristow, J. and Black, B. L. (2005). Gata4 expression in lateral mesoderm is downstream of BMP4 and is activated directly by forkhead and GATA transcription factors through a distal enhancer element. *Development* **132**, 3405-3417.

Rossi, J. M., Dunn, N. R., Hogan, B. L. M. and Zaret, K. S. (2001). Distinct mesodermal signals, including BMPs from the septum transversum mesenchyme, are required in combination for hepatogenesis from the endoderm. *Genes Dev.* **15**, 1998-2009.

Sequeira, I. and Nicolas, J.-F. (2012). Redefining the structure of the hair follicle by 3D clonal analysis. *Development* **139**, 3741-3751.

Sladek, F. M. (1993). Orphan receptor HNF-4 and liver-secific gene expression. *Receptor* **3**, 223-232.

Sosa-Pineda, B., Wigle, J. T. and Oliver, G. (2000). Hepatocyte migration during liver development requires Prox1. *Nat. Genet.* **25**, 254-255.

Stanger, B. Z., Tanaka, A. J. and Melton, D. A. (2007). Organ size is limited by the number of embryonic progenitor cells in the pancreas but not the liver. *Nature* **445**, 886-891.

Tajbakhsh, S., Bober, E., Babinet, C., Pournin, S., Arnold, H. and Buckingham, M. (1996). Gene targeting the *myf-5* locus with nlacZ reveals expression of this myogenic factor in mature skeletal muscle fibres as well as early embryonic muscle. *Dev. Dyn.* **206**, 291-300.

Tremblay, K. D. and Zaret, K. S. (2005). Distinct populations of endoderm cells converge to generate the embryonic liver bud and ventral foregut tissues. *Dev. Biol.* **280**, 87-99.

Tzouanacou, E., Wegener, A., Wymeersch, F. J., Wilson, V. and Nicolas, J.-F. (2009). Redefining the progression of lineage segregations during mammalian embryogenesis by clonal analysis. *Dev. Cell* **17**, 365-376.

Vassy, J., Kraemer, M., Chalumeau, M. T. and Foucrier, J. (1988). Development of the fetal rat liver: ultrastructural and stereological study of hepatocytes. *Cell Diff.* **24**, 9-24.

Zhao, R. and Duncan, S. A. (2005). Embryonic development of the liver. *Hepatology* **41**, 956-967.

SUPPLEMENTARY MATERIALS

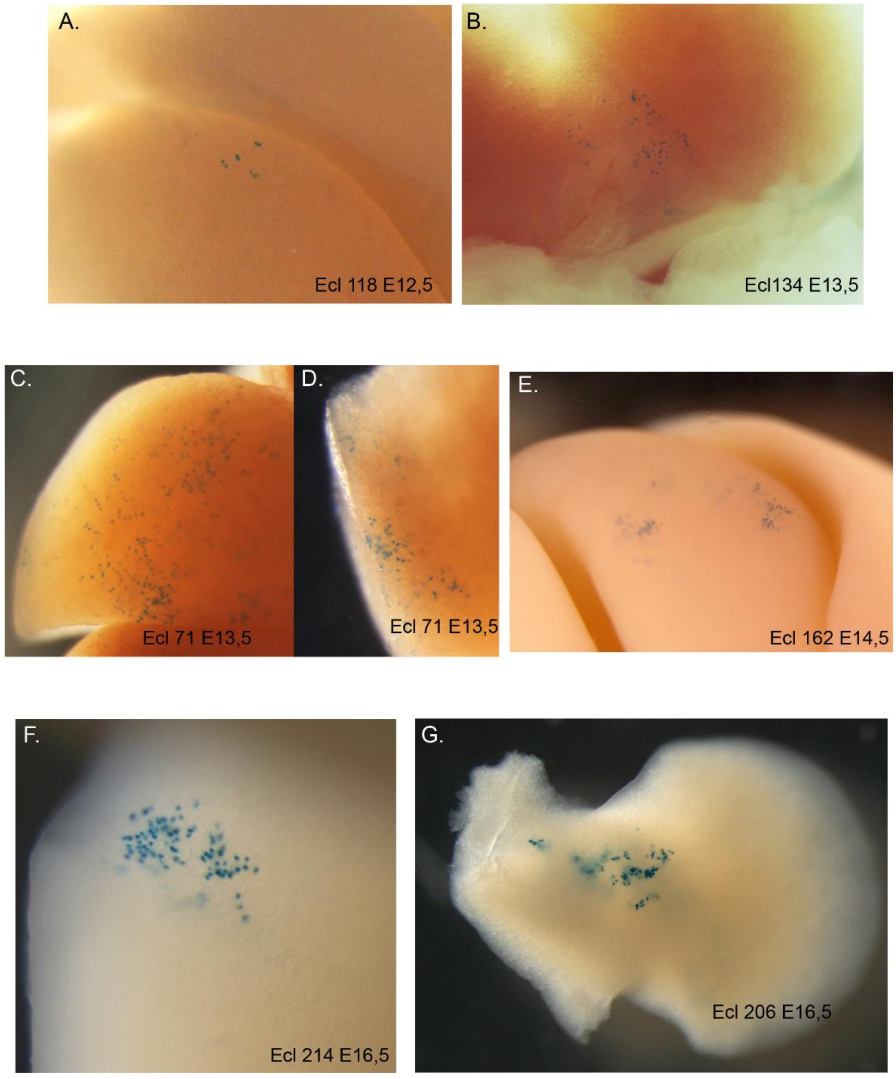

Fig. S1. **A**. Ecl 118 (E 12.5) shows 4 groups of 2 cells, located near the ventral wall of the LL lobe near to its meeting with the LM lobe. **B**. Ecl 134 (E13.5) where 136 blue nuclei can be counted using the microscope; these cells are located on the lower edge of the RM. **C, D**. Ecl 71 (E13.5) is particularly large (287 cells counted) and is seen both on the lateral (**C**) and caudal (**D**) surfaces of the LM. **E**. Ecl 162 (E14.5) occupies two areas of the RL comprising 182 cells. **F**. Ecl 214 (E16.5) is on the lateral edge of the caudate lobe, which emerges from and lies under the RL.**G**. Ecl 206 (E16.5) occupies nearly half of the newly emerging paddle-shaped papillary process, a very small lobe that develops on the central under side of both the left and right portions of the liver, but is derived from the RL. Stripes are present; 137 cells were counted. Lobe abbreviations: L, left or lateral; M, medial; R, right; C, caudate; PP, papillary process.

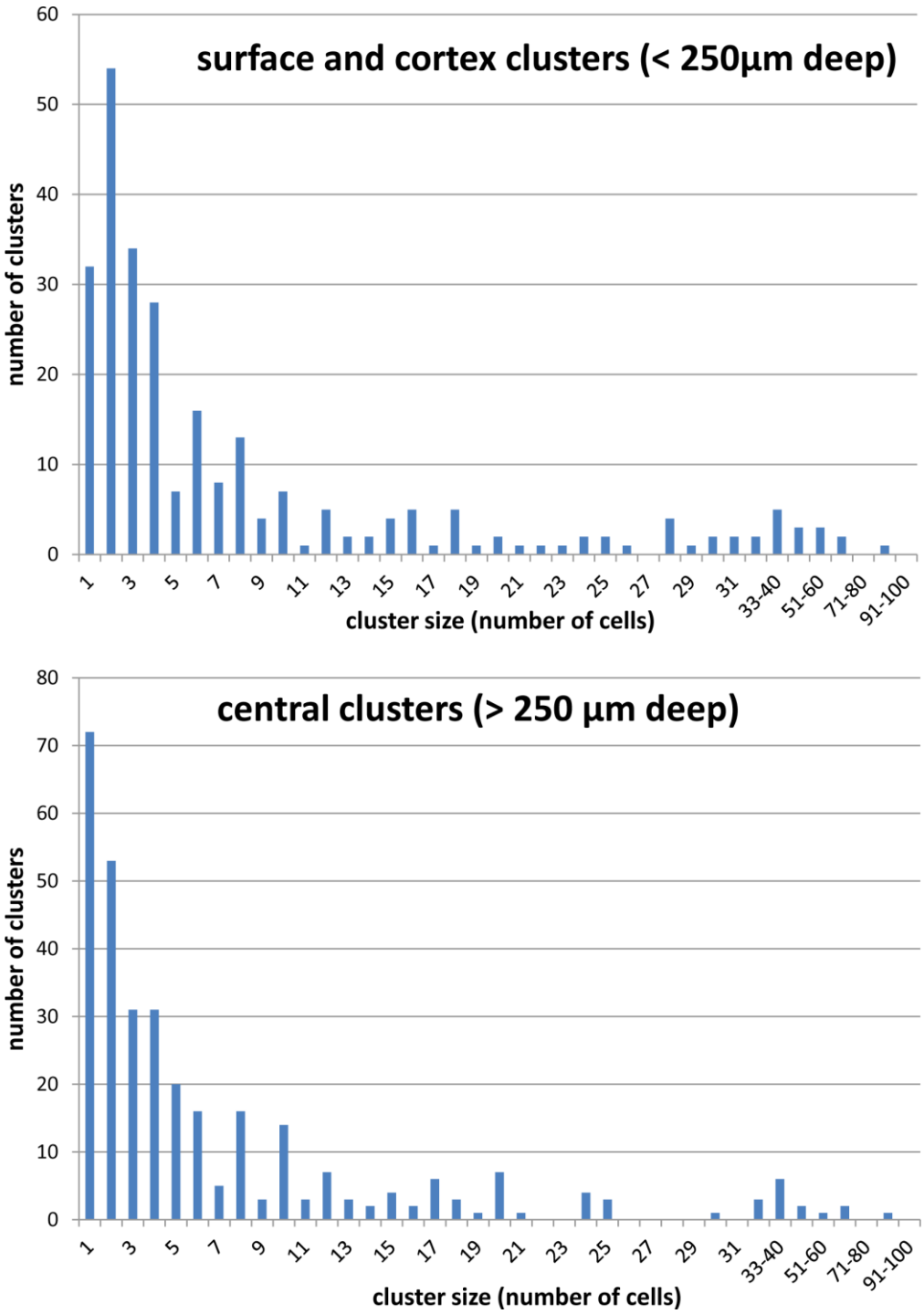

Fig. S2 Comparison of the frequency and size of clusters deep within the liver to those visible from the surface. All sections were counted, and the clusters were divided into two classes: those that were located at the surface and within 250-300µm of the surface, and those that were more deeply embedded within the section. The histograms depict the sizes of clusters and the numbers encountered either at/near the surface or deep within the section.

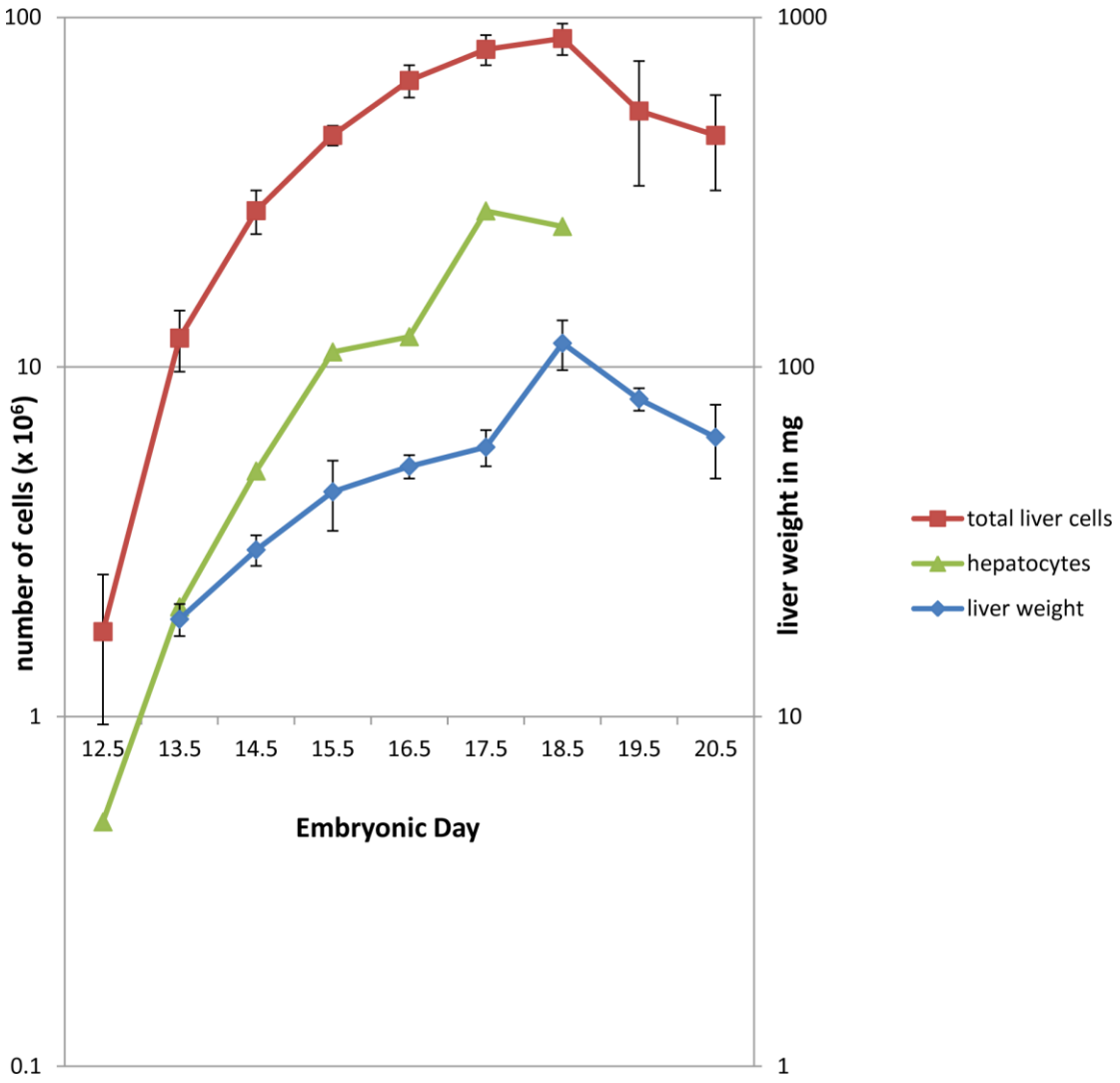

Fig. S3. Growth curves used to calculate average generation times during different phases of liver development. The values were calculated from tables presented in Paul et al., 1969 (Tables 1 and 2). Vassy et al. (1988) present a morphometric and stereological analysis of the developing rat liver between days 12 and 20: the volumetric fractions of hepatocyte nuclei permit us to plot the slope of hepatocyte growth, from which generation times can be deduced (Table 2 and embryonic liver weights given in the text). Three growth curves are shown: of total cells in the liver (squares), of hepatocytes (triangles), and weights of the embryonic livers (diamonds; scale in mg on the right).

Paul et al. (1969) counted total cells per liver using a trypsinized single-cell suspension of whole embryonic liver from E12.5 to E18.5 Swiss mice, and used cytocentrifugation and May-Grunwald Giemsa staining to prepare material for differential counts of the cell types. Liver weights were also determined. Vassy et al. (1988) have carried out stereological and morphometric analysis on livers of E12 to E18 Wistar rat embryos. The values of interest to us were total volumes of the livers and the volumetric fractions of hepatocyte nuclei (measured on electron micrographs), which permitted us to establish the slope of the nuclear increments with time on a logarithmic scale. This avoided the necessity of correcting for increase in the cytoplamsmic volume of hepatoblasts/hepatocytes during development. The slopes obtained from data of Vassy etl al. (1988) were very similar to those of counts of hepatocytes by Paul et al. (1969), after correction for the developmental stage of E days for the rat compared to the mouse (Kaufman, 1992). The slopes for the rat are not shown in the figures because of the differences in timing of development of the two species.

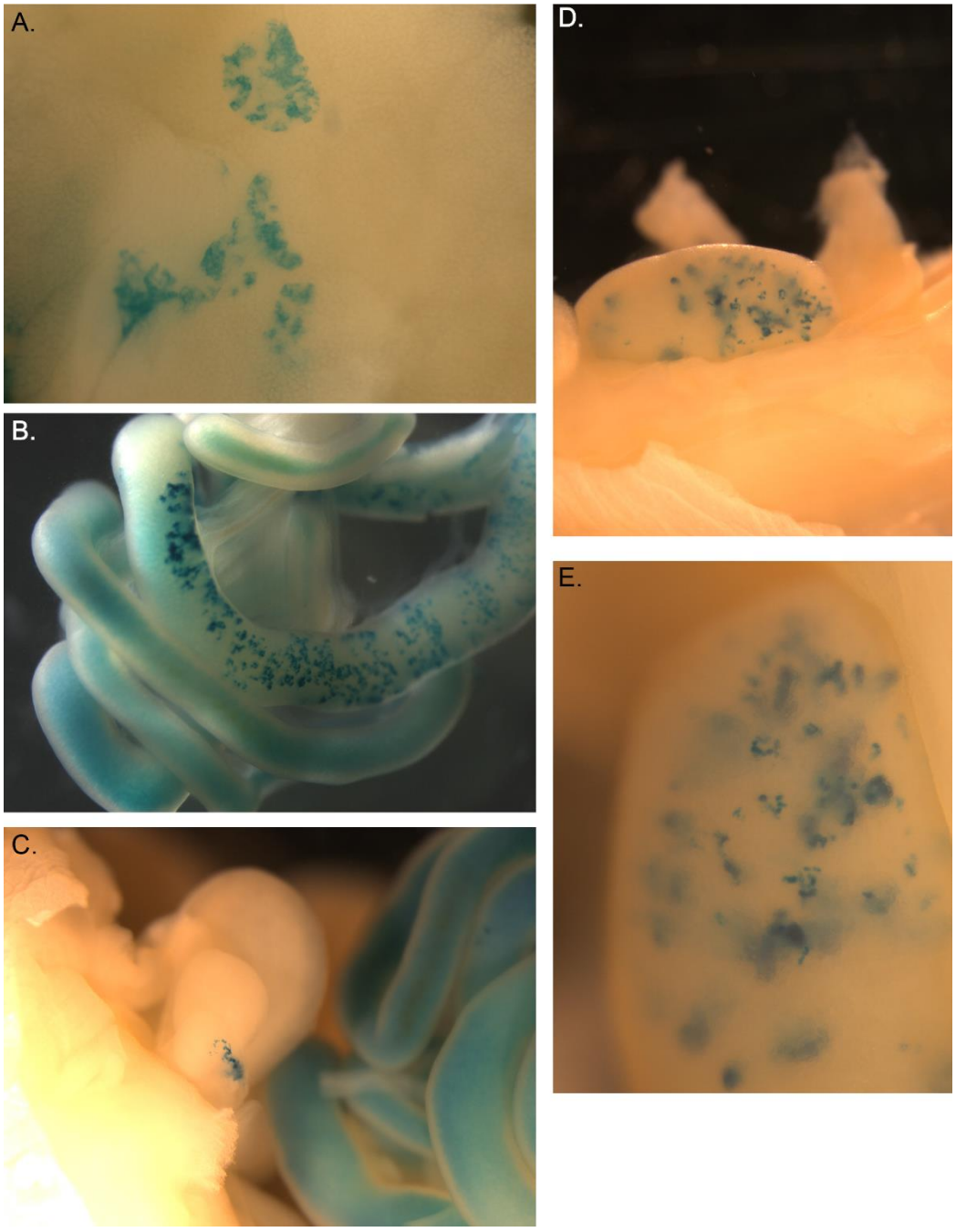

Fig. S4. Labeled clusters in non-liver tissues that express HNF4α. A. Pancreas (40X), 3 week old mouse. B. Large intestine (E 17.5 embryo); 8X C. Testis (E16.50; the labeled tissue is the epidydimus (8X). D and E. Kidney (E16.5) (8X and 25X respectively). The convoluted tubules contain HNF4α.